

$^{12}\text{C} + ^{16}\text{O}$ molecular resonances at deep sub-barrier energy

Yasutaka Taniguchi*

*Department of Information Engineering,
National Institute of Technology (KOSEN),
Kagawa College, Mitoyo, Kagawa 769-1192, Japan*

Masaaki Kimura[†]

*Department of Physics, Hokkaido University,
Sapporo, Hokkaido 060-0810, Japan and
Nuclear Reaction Data Centre, Hokkaido University,
Sapporo, Hokkaido 060-0810, Japan*

(Dated: September 2, 2019)

Abstract

The existence of $^{12}\text{C} + ^{16}\text{O}$ molecular resonances at sub-barrier energy has been a significant problem in nuclear astrophysics because they strongly affect the $^{12}\text{C} + ^{16}\text{O}$ fusion reaction rate in type Ia supernovae and heavy stars. However, experimental surveys have been limited to 4 MeV and cannot access the deep sub-barrier energy due to a very small fusion cross section. Here we predict a couple of resonances with $J^\pi = 0^+, 2^+$, and 4^+ in the deep sub-barrier energy based on the antisymmetrized molecular dynamics calculation that reproduces the known resonances and low-lying spectrum of ^{28}Si .

Introduction.— Understanding the origin of matter is a significant challenge in nuclear and astrophysics fields. The $^{12}\text{C} + ^{16}\text{O}$ fusion reaction at thermal energy is critical for nucleosynthesis in type Ia supernovae and heavy stars. The ignition of type Ia supernovae is carbon and oxygen burning, and this strongly influences the abundance of elements in the $14 \lesssim Z \lesssim 20$ region [1]. If they exist, $^{12}\text{C} + ^{16}\text{O}$ molecular resonances close to the Gamow window increase the cross-section in order of magnitude. Therefore, searching for molecular resonances and determining their resonance parameters are of primary importance for understanding of the reaction rate.

Experimentally, resonances at 3.9–4.0 and 4.4 MeV have been observed by low-energy $^{12}\text{C} + ^{16}\text{O}$ fusion reaction, and an increased $^{12}\text{C} + ^{16}\text{O}$ fusion reaction rate has been reported previously [2]. In addition, resonances at a higher energy region have also been observed by radiative capture reactions [3, 4] and other reactions [5]. Thus, many experiments have been performed to identify the resonances at thermal energy; however, resonances at deep sub-barrier energy are still unclear.

For this problem, theoretical studies are far from satisfactory although a number of cluster model calculations have been performed. For example, Baye *et al.* performed a resonating group method (RGM) calculation for $^{12}\text{C} + ^{16}\text{O}$ system and obtained two positive parity rotational bands [6, 7], one of which is just above the $^{12}\text{C} + ^{16}\text{O}$ threshold and may have some influence on the reaction rate. Katō *et al.* performed an orthogonality condition model (OCM) calculation including both elastic and inelastic channels ($^{12}\text{C}(0_1^+, 2_1^+, 4_1^+)$ states) [8]. They demonstrated the existence of a much greater number of the molecular states compared to the RGM calculation, likely owing to elastic and inelastic channel mixing. Kanada-En'yo *et al.* reported the existence of three positive-parity $^{12}\text{C} + ^{16}\text{O}$ molecular bands based on the antisymmetrized molecular dynamics (AMD) calculation without a priori assumption of the $^{12}\text{C} + ^{16}\text{O}$ cluster structure [9]. Similar to the RGM calculation, one of molecular bands is close to the $^{12}\text{C} + ^{16}\text{O}$ threshold. Thus, many calculations have been performed; however, the number of molecular resonances and their energies are quite different according to theoretical models. This uncertainty comes from the ambiguity of effective nucleon-nucleon interactions and limitation of their model space.

To overcome this problem, we performed the AMD calculation using the effective Gogny D1S interaction [10]. This calculation has already been performed for the low-lying states of ^{28}Si (the composite system of $^{12}\text{C} + ^{16}\text{O}$ cluster) [11]. It reasonably described both the

oblately deformed ground-state band and a prolate normal-deformed (ND) band. Furthermore, it predicted a superdeformed (SD) band having large overlap with the $\alpha + {}^{24}\text{Mg}$ cluster configuration, which was subsequently identified experimentally [12]. In this study, we extend this calculation to the highly excited states to identify ${}^{12}\text{C} + {}^{16}\text{O}$ molecular resonances. To cover the broad model space required to study ${}^{12}\text{C} + {}^{16}\text{O}$ resonances, we introduce a constraint on the inter-cluster distances which enables us to describe various cluster configurations.

Theoretical framework.— We employ the AMD framework [13–16] with the Gogny D1S effective interaction [10], which successfully described the low-lying and superdeformed states of ${}^{28}\text{Si}$ [11]. The basis wave function of AMD is a parity-projected Slater determinant of the single-particle wave packets,

$$\begin{aligned} \Phi_{\text{int}}^{\pi} &= \frac{1 + \pi P_x}{2} \mathcal{A} \{ \varphi_1, \dots, \varphi_A \}, \\ \varphi_i &= \prod_{\sigma=x,y,z} \left(\frac{2\nu_{\sigma}}{\pi} \right)^{1/4} \exp \{ -\nu_{\sigma} (r_{\sigma} - Z_{i\sigma})^2 \} \\ &\quad \times (\alpha_i |\xi_{\uparrow}\rangle + \beta_i |\xi_{\downarrow}\rangle) \times (|p\rangle \text{ or } |n\rangle), \end{aligned} \quad (1)$$

$$(2)$$

where each wave packet φ_i has the following parameters: Gaussian centroid \mathbf{Z}_i , width parameter $\boldsymbol{\nu}$ and spin direction α_i and β_i . Note that isospin part is fixed to either of proton (p) or neutron (n). Here, $\boldsymbol{\nu}$ is a real vector, and the other parameters are complex numbers. All parameters are determined by the energy variation with two different constraints. The first is a constraint on the quadrupole deformation and the second is on the inter-cluster distance d between ${}^{12}\text{C}$ - ${}^{16}\text{O}$ clusters, and between α - ${}^{24}\text{Mg}$ clusters. The constraint on the inter-cluster distance naturally yields the clustered basis wave functions handling the cluster polarization effect [17]. After energy variation, the basis wave functions are projected to the eigenstates of the angular momentum and superposed to diagonalize the nuclear Hamiltonian.

The obtained wave functions of ${}^{28}\text{Si}$ are an admixture of the ${}^{12}\text{C} + {}^{16}\text{O}$ cluster, $\alpha + {}^{24}\text{Mg}$ cluster and non-cluster wave functions. To identify the ${}^{12}\text{C} + {}^{16}\text{O}$ molecular states, we calculated the reduced width amplitude (RWA), which is the probability amplitude to find the clusters at the inter-cluster distance a : thus, the RWA is a good measure for clustering. It is defined as follows:

$$y_l(a) = \sqrt{\frac{28!}{12!16!}} \left\langle \frac{\delta(r-a)}{r^2} \Phi_{12\text{C}} \Phi_{16\text{O}} Y_l(\hat{r}) \left| \Psi_{28\text{Si}}^l \right. \right\rangle, \quad (3)$$

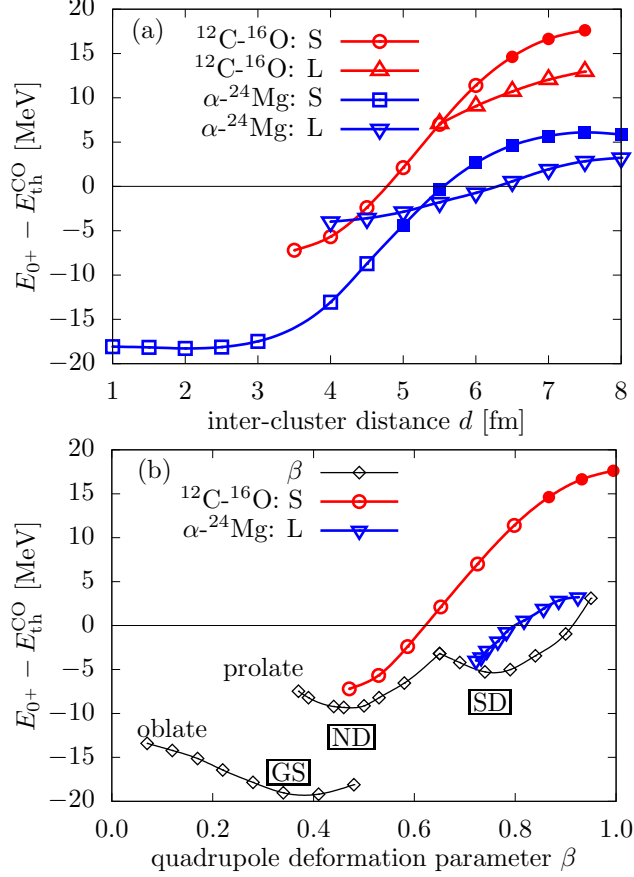


FIG. 1. Energy curves of the $J^\pi = 0^+$ state obtained by energy variation with constraints. (a) Energy curves for the $^{12}\text{C} + ^{16}\text{O}$ and $\alpha + ^{24}\text{Mg}$ cluster systems as functions of inter-cluster distance. Two different configurations of clusters are calculated (denoted S- and L-type). (b) Energy curve obtained by the constraint on the quadrupole deformation as a function of deformation parameter β compared to the energy curves for the cluster configurations shown in panel (a).

where the bra state is the reference cluster state, in which the ^{12}C ($\Phi_{^{12}\text{C}}$) and ^{16}O ($\Phi_{^{16}\text{O}}$) clusters are coupled to angular momentum l with inter-cluster distance a . The ket state is the wave function of ^{28}Si calculated by AMD. Here, $\Phi_{^{12}\text{C}}$ and $\Phi_{^{16}\text{O}}$ are the $(0s)^4(0p_{3/2})^8$ [18] and $(0s)^4(0p)^{12}$ configurations of the harmonic oscillator potential, respectively. In practical calculation, Eq. (3) was estimated using an approximate method [19].

Results and discussions.— Figure 1 (a) shows the energy curves obtained by the energy variation with the constraint on inter-cluster distance d . Energies are measured from $^{12}\text{C} + ^{16}\text{O}$ threshold energy that is determined by the energy variation of the AMD wave functions of ^{12}C and ^{16}O clusters after parity projection. For each of the $^{12}\text{C} + ^{16}\text{O}$ and $\alpha + ^{24}\text{Mg}$

cluster systems, two different configurations (denoted S-type and L-type) were obtained. In the S-type configuration, the spherical clusters (*i.e.*, ^{16}O and α) are located on the short axis of the deformed clusters (*i.e.*, ^{12}C and ^{24}Mg). In the L-type configuration, they are located on the long axis. At larger inter-cluster distance ($d > 5.5$ fm), the L-type configurations have smaller energy due to the larger overlap between clusters. The S-type cluster wave functions with long inter-cluster distance were prepared by shifting cluster position in the S-type wave functions with $d = 6$ and 4.5 fm for the $^{12}\text{C}-^{16}\text{O}$ and $\alpha-^{24}\text{Mg}$ wave functions, respectively. The figure also shows that the Coulomb barrier height for the $^{12}\text{C}+^{16}\text{O}$ system was estimated as approximately 10 MeV above the $^{12}\text{C}+^{16}\text{O}$ threshold. This estimation reasonably coincides with a simple formula, $V_c = \alpha Z_1 Z_2 / (R_1 + R_2)$, where α , Z_1 , Z_2 , R_1 and R_2 denote the fine structure constant, the charges of the clusters, and the radii of the clusters, respectively.

Panel (b) shows the energy curve obtained by the constraint on the quadrupole deformation parameter β . It has three minima denoted GS, ND, and SD, which are the dominant components of the ground-state, ND, and SD bands, respectively [11]. The figure also shows the energy curves for the S-type $^{12}\text{C} + ^{16}\text{O}$ and L-type $\alpha + ^{24}\text{Mg}$ cluster systems which are same as those shown in panel (a), but plotted as the functions of β . The energy of these cluster configurations become close to the ND and SD minima at shorter inter-cluster distance, which indicates the large overlap between the ND and $^{12}\text{C} + ^{16}\text{O}$ cluster configurations, and between the SD and $\alpha + ^{24}\text{Mg}$ cluster configurations. In fact, it was found that the wave functions at the ND and SD configurations have non-negligible contributions to the molecular states.

The GCM calculation was performed by superposing these basis wave functions. As discussed in Ref. 11, it reasonably described the low-lying states, *i.e.*, the oblate-deformed ground band and prolate ND band. It also predicted the SD band, which was confirmed experimentally [12]. Following these results, in this study, we focus on the $^{12}\text{C}+^{16}\text{O}$ molecular states, which are of astrophysical interest. For this purpose, we selected the excited states with large RWA for $^{12}\text{C} + ^{16}\text{O}$ clustering. Figure 2 summarizes the obtained levels classified as the $^{12}\text{C} + ^{16}\text{O}$ molecular states. They are denoted ND, SD, MR1 and MR2 bands, and their properties are as follows:

- (1) MR1: A group of the highly excited states, which lie at 5 to 10 MeV in the case of the $J^\pi = 0^+$ states, with huge RWA that have a peak at $a = 6-7$ fm (Fig. 3). We

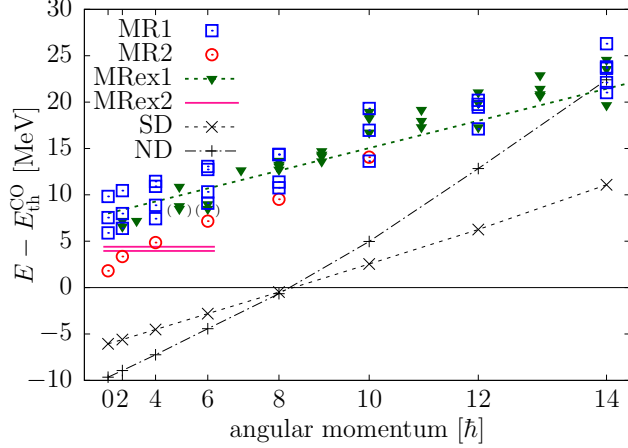


FIG. 2. Level scheme of the excited states with large $^{12}\text{C} + ^{16}\text{O}$ RWA. MR1 and MR2 are the calculated $^{12}\text{C} + ^{16}\text{O}$ molecular resonances which, respectively, correspond to the observed resonances denoted MRex1 [3–5] and MRex2 [2]. ND and SD denote normal deformed and superdeformed bands, respectively.

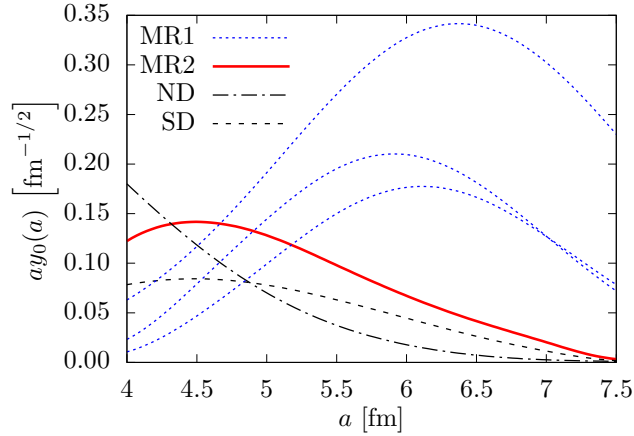


FIG. 3. The RWA of the $J^\pi = 0^+$ states of MR1, MR2, ND, and SD bands for $^{12}\text{C} + ^{16}\text{O}$ clustering.

identified these states as molecular resonances (MR1). The energy and moment-of-inertia of MR1 agree with the molecular resonances observed by the $^{12}\text{C}(^{16}\text{O}, ^{28}\text{Si}^*)$ and $^{24}\text{Mg}(\alpha, ^{12}\text{C})^{16}\text{O}$ reactions (triangles and dotted line in Fig. 2) fairly well. Note that no other microscopic calculations have explained the observed molecular resonance.

The Coulomb barrier height is approximately 10 MeV; thus, these states are considered as the barrier-top resonances. Due to the pronounced clustering, the $B(E2)$ strength between the $J^\pi \leq 6^+$ states are in the order of $10^3 \text{ e}^2\text{fm}^4$ and much stronger than other states (Fig. 4). The $B(E2)$ strengths also suggests that the MR1 states with

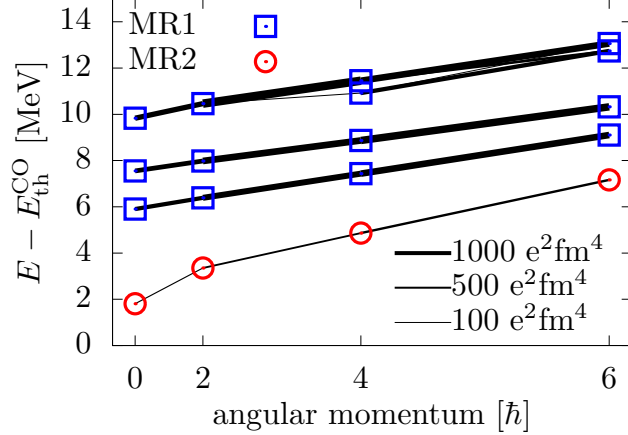


FIG. 4. $B(E2)$ transition strengths of MR1 and MR2 bands. The Widths of lines connecting those states are proportional to $B(E2)$ values.

$J^\pi \leq 6^+$ can be classified into three rotational bands. However, we also found that the inter-band transitions become very strong for the $J^\pi > 6^+$ states and the band assignment is rather ambiguous for high-spin states.

- (2) MR2: In addition to MR1, we found another molecular band which we denote MR2. MR2 is built on the 0^+ state just above the threshold (1.8 MeV). The energy of this band is significantly less than the Coulomb barrier (deep sub-barrier); thus, the RWA of this band is less than the MR1 states but greater than the ND and SD bands (Fig. 3). Furthermore, the peak position of RWA is at shorter distance ($a = 4.5$ fm), which suggests a compact $^{12}\text{C} + ^{16}\text{O}$ resonances. Reflecting this, the $B(E2)$ strengths and moment-of-inertia are smaller than MR1. The energy of this band is within the Gamow window of the Carbon burning process; therefore, it is likely to have an impact on the $^{12}\text{C} + ^{16}\text{O}$ fusion reaction rate in the stellar environment. Interestingly, Fang *et al.* reported the existence of the resonances at 3.9–4.0 and 4.4 MeV in a low-energy $^{12}\text{C} + ^{16}\text{O}$ fusion reaction experiment [2], which reasonably coincide with the 2^+ and 4^+ states of MR2 band. A more detailed study of this band will be important to understand of the $^{12}\text{C} + ^{16}\text{O}$ fusion reaction rate, which affects the abundance of elements in the $14 \lesssim Z \lesssim 20$ region [1].

- (3) The ND band built on the prolately deformed 0_3^+ state has overlap with the S-type $^{12}\text{C} + ^{16}\text{O}$ configuration; however, the RWA of this band is not as large as the MR1 and

MR2 due to the deeper binding. In this band, the cluster configuration is considerably distorted by the formation of the prolately deformed mean-field. Nevertheless, this band may be classified as the lowest Pauli-allowed $^{12}\text{C} + ^{16}\text{O}$ molecular band because no other low-lying states have large $^{12}\text{C} + ^{16}\text{O}$ RWA.

- (4) Unexpectedly, the SD band, which is predominated by the L-type $\alpha + ^{24}\text{Mg}$ cluster configuration, also has non-negligible $^{12}\text{C} + ^{16}\text{O}$ RWA that is even greater than the ND band at the long inter-cluster distance as shown in Fig. 3, which shows the strong mixing of the $\alpha + ^{24}\text{Mg}$ and $^{12}\text{C} + ^{16}\text{O}$ cluster channels. Note that this mixing characteristic reasonably agrees with the observation, *i.e.*, it has been reported that the observed SD states are strongly populated in all of the $^{12}\text{C}(^{20}\text{Ne}, \alpha)^{28}\text{Si}$ [12, 20], $^{24}\text{Mg}(^6\text{Li}, d)^{28}\text{Si}$ [21] and $^{24}\text{Mg}(\alpha, \gamma)^{28}\text{Si}$ [22–24] reactions. Thus, the present calculation provides further evidence for the SD band in ^{28}Si and its cluster nature.

In short, we predict the existence of the deep sub-barrier $^{12}\text{C} + ^{16}\text{O}$ molecular states based on the AMD calculation which reasonably reproduces the known low-lying states, the SD band and $^{12}\text{C} + ^{16}\text{O}$ molecular resonances.

Conclusions. — In summary, the $^{12}\text{C} + ^{16}\text{O}$ molecular resonances were investigated using the AMD framework. By superposition of the wave functions of the $^{12}\text{C}-^{16}\text{O}$ and $\alpha-^{24}\text{Mg}$ clusters and non-cluster states, the low-lying and superdeformed bands and the known $^{12}\text{C} + ^{16}\text{O}$ molecular resonances were reproduced reasonably. Furthermore, the calculation predicted the extremely low-energy $^{12}\text{C} + ^{16}\text{O}$ resonances close to the $^{12}\text{C} + ^{16}\text{O}$ threshold. Some of these $^{12}\text{C} + ^{16}\text{O}$ resonances are the candidates of the resonances observed by the low-energy $^{12}\text{C} + ^{16}\text{O}$ fusion reactions and are expected to have great impact on stellar reactions.

This work was supported by the Hattori Hokokai Foundation Grant-in-Aid for Technological and Engineering Research, a grant for the RCNP joint research project, the collaborative research program 2018/2019 at Hokkaido University, and JSPS KAKENHI Grant No. 19K03859. Numerical calculations were performed using Oakforest-PACS at the CCS, University of Tsukuba, and XC40 at YITP, Kyoto University.

* taniguchi-y@di.kagawa-nct.ac.jp

† masaaki@nucl.sci.hokudai.ac.jp

- [1] H. Martínez-Rodríguez, C. Badenes, H. Yamaguchi, E. Bravo, F. X. Timmes, B. J. Miles, D. M. Townsley, A. L. Piro, H. Mori, B. Andrews, and S. Park, *Astrophys. J.* **843**, 35 (2017).
- [2] X. Fang, W. P. Tan, M. Beard, R. J. deBoer, G. Gilardy, H. Jung, Q. Liu, S. Lyons, D. Robertson, K. Setoodehnia, C. Seymour, E. Stech, B. Vande Kolk, M. Wiescher, R. T. deSouza, S. Hudan, V. Singh, X. D. Tang, and E. Uberseder, *Phys. Rev. C* **96**, 045804 (2017).
- [3] N. I. Ashwood, J. T. Murgatroyd, N. M. Clarke, M. Freer, B. R. Fulton, A. St. J. Murphy, S. P. G. Chappell, R. L. Cowin, G. K. Dillon, D. L. Watson, W. N. Catford, N. Curtis, M. Shawcross, and V. Pucknell, *Phys. Rev. C* **63**, 034315 (2001).
- [4] A. Goasduff, S. Courtin, F. Haas, D. Lebhertz, D. G. Jenkins, J. Fallis, C. Ruiz, D. A. Hutcheon, P.-A. Amandruz, C. Davis, U. Hager, D. Ottewell, and G. Ruprecht, *Phys. Rev. C* **89**, 014305 (2014).
- [5] N. Cindro, *La Rivista del Nuovo Cimento* **4**, 1 (1981).
- [6] D. Baye, *Nucl. Phys. A* **272**, 445 (1976).
- [7] D. Baye and P. H. Heenen, *Nucl. Phys. A* **283**, 176 (1977).
- [8] K. Katō, S. Okabe, and Y. Abe, *Prog. Theor. Phys.* **74**, 1053 (1985).
- [9] Y. Kanada-En'yo, M. Kimura, and H. Horiuchi, *Nucl. Phys. A* **738**, 3 (2004).
- [10] J. Berger, M. Girod, and D. Gogny, *Comput. Phys. Commun.* **63**, 365 (1991).
- [11] Y. Taniguchi, Y. Kanada-En'yo, and M. Kimura, *Phys. Rev. C* **80**, 044316 (2009).
- [12] D. G. Jenkins, C. J. Lister, M. P. Carpenter, P. Chowdury, N. J. Hammond, R. V. F. Janssens, T. L. Khoo, T. Lauritsen, D. Seweryniak, T. Davinson, P. J. Woods, A. Jokinen, H. Penttila, F. Haas, and S. Courtin, *Phys. Rev. C* **86**, 064308 (2012).
- [13] Y. Kanada-En'yo and H. Horiuchi, *Prog. Theor. Phys.* **93**, 115 (1995).
- [14] A. Doté, H. Horiuchi, and Y. Kanada-En'yo, *Phys. Rev. C* **56**, 1844 (1997).
- [15] M. Kimura, *Phys. Rev. C* **69**, 044319 (2004).
- [16] M. Kimura, T. Suhara, and Y. Kanada-En'yo, *The European Physical Journal A* **52**, 373 (2016).
- [17] Y. Taniguchi, M. Kimura, and H. Horiuchi, *Prog. Theor. Phys.* **112**, 475 (2004).
- [18] T. Suhara, N. Itagaki, J. Cseh, and M. Płoszajczak, *Phys. Rev. C* **87**, 054334 (2013).
- [19] Y. Kanada-En'yo, T. Suhara, and Y. Taniguchi, *Prog. Theor. Exp. Phys.* **2014**, 073D02 (2014).
- [20] S. Kubono, K. Morita, M. H. Tanaka, A. Sakaguchi, M. Sugitani, and S. Kato, *Nucl. Phys. A* **457**, 461 (1986).
- [21] T. Tanabe, M. Yasue, K. Sato, K. Ogino, Y. Kadota, Y. Taniguchi, K. Obori, K. Makino,

- and M. Tochi, Phys. Rev. C **24**, 2556 (1981).
- [22] J. Brenneisen, D. Grathwohl, M. Lickert, R. Ott, H. Röpke, J. Schmälzlin, P. Siedle, and B. H. Wildenthal, Z. Phys. A **352**, 149 (1995).
- [23] J. Brenneisen, D. Grathwohl, M. Lickert, R. Ott, H. Röpke, J. Schmälzlin, P. Siedle, and B. H. Wildenthal, Z. Phys. A **352**, 279 (1995).
- [24] J. Brenneisen, D. Grathwohl, M. Lickert, R. Ott, H. Röpke, J. Schmälzlin, P. Siedle, and B. H. Wildenthal, Z. Phys. A **352**, 403 (1995).